

## Nanoparticle-Directed Self-Assembly of Amphiphilic Block Copolymers

Amanda C. Kamps,<sup>†</sup> Brenda L. Sanchez-Gaytan,<sup>†</sup> Robert J. Hickey,<sup>†</sup> Nigel Clarke,<sup>‡</sup> Michael Fryd,<sup>†</sup> and So-Jung Park\*,<sup>†</sup>

<sup>†</sup>Department of Chemistry, University of Pennsylvania, Philadelphia, Pennsylvania 19104, and

<sup>‡</sup>Department of Chemistry, Durham University, Durham DH1 3LE, U.K.

Received June 23, 2010

Nanoparticles can form unique cavity-like structures in core–shell type assemblies of block copolymers through the cooperative self-assembly of nanoparticles and block copolymers. We show that the self-assembly behavior is general for common as-synthesized alkyl-terminated nanoparticles for a range of nanoparticle sizes. We examined various self-assembly conditions such as solvent compositions, nanoparticle coordinating ligands, volume fraction of nanoparticles, and nanoparticle sizes in order to elucidate the mechanism of the radial assembly formation. These experiments along with strong segregation theory calculations indicated that both the enthalpic interaction and the polymer stretching energy are important factors in the coassembly formation. The slightly unfavorable interaction between the hydrophobic segment of polymers and alkyl-terminated nanoparticles causes the accumulation of nanoparticles at the interface between the polymer core and the shell, forming the unique cavity-like structure. The coassemblies were stabilized for a limited range of nanoparticle volume fractions within which the inclusion of nanoparticle layers reduces the polymer stretching. The volume fraction range yielding the well-defined radial coassembly structure was mapped out with varying nanoparticle sizes. The experimental and theoretical phase map provides the guideline for the coassembly formation of as-synthesized alkyl-terminated nanoparticles and amphiphilic block copolymers.

For the past decade, there has been a considerable effort toward combining nanoparticles and polymers in materials synthesis and device fabrication in order to take advantage of the unique physical properties of nanoparticles and the excellent processability of polymers.<sup>1–6</sup> An important issue in this area is to develop efficient ways to control the arrangement of nanoparticles in polymer matrix because the dispersion of nanoparticles significantly impacts the electronic, transport, and mechanical properties of the composite materials.<sup>7,8</sup> Recently, it has been shown that the cooperative self-assembly of nanoparticles and block copolymers can produce a range of well-ordered arrays of nanoparticles in polymer thin films.<sup>9,10</sup> In this approach, nanoparticles are segregated into a favorable polymer domain or to the

interface between polymer domains, and the arrangement of nanoparticles can be directed by controlling the interaction between nanoparticles and polymers.<sup>11,12</sup>

In the solution phase, the self-assembly of block copolymers and nanoparticles has been explored as a promising synthetic tool for generating multifunctional nanostructures.<sup>13–20</sup> In particular, Taton and co-workers have developed a simple way to prepare well-defined, water-soluble multicomponent nanoparticles by the self-assembly of nanoparticles of varying compositions and amphiphilic block copolymers composed of polystyrene and poly(acrylic acid) (PAA-*b*-PS).<sup>15,16,18</sup> The self-assembly process produced block copolymer micelles encapsulating various types of nanoparticles in the hydrophobic core of the micelles, where

\*To whom correspondence should be addressed. E-mail: sojungp@sas.upenn.edu.

(1) Balazs, A. C.; Emrick, T.; Russell, T. P. Nanoparticle polymer composites: Where two small worlds meet. *Science* **2006**, *314*, 1107–1110.

(2) Saunders, B. R.; Turner, M. L. Nanoparticle-polymer photovoltaic cells. *Adv. Colloid Interface Sci.* **2008**, *138*, 1–23.

(3) Yang, J.; Dave, S. R.; Gao, X. H. Quantum dot nanobarcodes: Epitaxial assembly of nanoparticle-polymer complexes in homogeneous solution. *J. Am. Chem. Soc.* **2008**, *130*, 5286–5292.

(4) Ofir, Y.; Samanta, B.; Rotello, V. M. Polymer and biopolymer mediated self-assembly of gold nanoparticles. *Chem. Soc. Rev.* **2008**, *37*, 1814–1823.

(5) Vaia, R. A.; Maguire, J. F. Polymer nanocomposites with prescribed morphology: Going beyond nanoparticle-filled polymers. *Chem. Mater.* **2007**, *19*, 2736–2751.

(6) Kang, Y. J.; Erickson, K. J.; Taton, T. A. Plasmonic nanoparticle chains via a morphological, sphere-to-string transition. *J. Am. Chem. Soc.* **2005**, *127*, 13800–13801.

(7) Kinge, S.; Crego-Calama, M.; Reinhardt, D. N. Self-assembling nanoparticles at surfaces and interfaces. *ChemPhysChem* **2008**, *9*, 20–42.

(8) Shenhar, R.; Norsten, T. B.; Rotello, V. M. Polymer-mediated nanoparticle assembly: Structural control and applications. *Adv. Mater.* **2005**, *17*, 657–669.

(9) Yeh, S. W.; Wei, K. H.; Sun, Y. S.; Jeng, U. S.; Liang, K. S. CdS nanoparticles induce a morphological transformation of poly(styrene-*b*-4-vinylpyridine) from hexagonally packed cylinders to a lamellar structure. *Macromolecules* **2005**, *38*, 6559–6565.

(10) Li, Q. F.; He, J. B.; Glogowski, E.; Li, X. F.; Wang, J.; Emrick, T.; Russell, T. P. Responsive assemblies: Gold nanoparticles with mixed ligands in microphase separated block copolymers. *Adv. Mater.* **2008**, *20*, 1462–1466.

(11) Chiu, J. J.; Kim, B. J.; Kramer, E. J.; Pine, D. J. Control of nanoparticle location in block copolymers. *J. Am. Chem. Soc.* **2005**, *127*, 5036–5037.

(12) Chung, H.; Ohno, K.; Fukuda, T.; Composto, R. J. Self-regulated structures in nanocomposites by directed nanoparticle assembly. *Nano Lett.* **2005**, *5*, 1878–1882.

(13) Gao, X. H.; Cui, Y. Y.; Levenson, R. M.; Chung, L. W. K.; Nie, S. M. In vivo cancer targeting and imaging with semiconductor quantum dots. *Nature Biotechnol.* **2004**, *22*, 969–976.

(14) Euliss, L. E.; Grancharov, S. G.; O'Brien, S.; Deming, T. J.; Stucky, G. D.; Murray, C. B.; Held, G. A. Cooperative assembly of magnetic nanoparticles and block copolyptides in aqueous media. *Nano Lett.* **2003**, *3*, 1489–1493.

(15) Kim, B. S.; Qiu, J. M.; Wang, J. P.; Taton, T. A. Magnetomicelles: Composite nanostructures from magnetic nanoparticles and cross-linked amphiphilic block copolymers. *Nano Lett.* **2005**, *5*, 1987–1991.

(16) Kim, B. S.; Taton, T. A. Multicomponent nanoparticles via self-assembly with cross-linked block copolymer surfactants. *Langmuir* **2007**, *23*, 2198–2202.

(17) Zhu, J. T.; Hayward, R. C. Spontaneous generation of amphiphilic block copolymer micelles with multiple morphologies through interfacial instabilities. *J. Am. Chem. Soc.* **2008**, *130*, 7496–7502.

(18) Kang, Y. J.; Taton, T. A. Core/shell gold nanoparticles by self-assembly and crosslinking of micellar, block-copolymer shells. *Angew. Chem., Int. Ed.* **2005**, *44*, 409–412.

(19) Jeon, S. J.; Yang, S. M.; Kim, B. J.; Petrie, J. D.; Jang, S. G.; Kramer, E. J.; Pine, D. J.; Yi, G. R. Hierarchically Structured Colloids of Diblock Copolymers and Au Nanoparticles. *Chem. Mater.* **2009**, *21*, 3739–3741.

(20) Yusuf, H.; Kim, W. G.; Lee, D. H.; Guo, Y. Y.; Moffitt, M. G. Size control of mesoscale aqueous assemblies of quantum dots and block copolymers. *Langmuir* **2007**, *23*, 868–878.

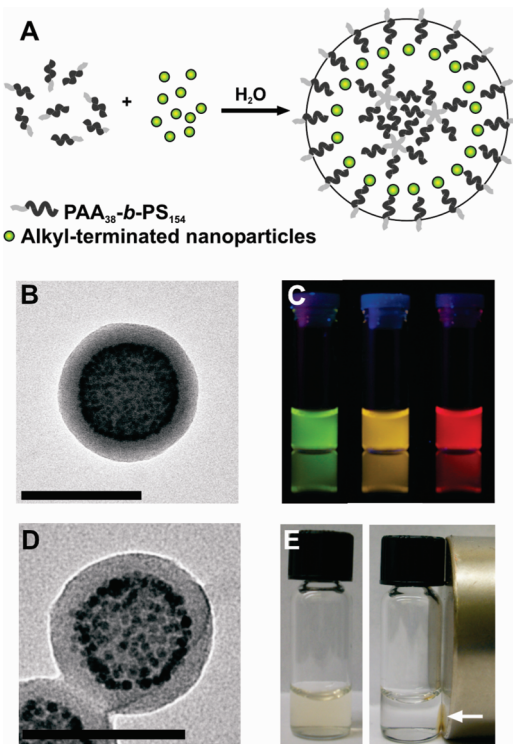


**Figure 1.** (A) Schematic depiction of the self-assembly of nanoparticles and block copolymers. (B) A TEM image of CdSe@ZnS nanoparticles ( $4.1 \pm 0.4$  nm) forming a cavity-like structure in block copolymer assemblies. (C) Aqueous solutions of block copolymer assemblies incorporated with CdSe@ZnS nanoparticles of different sizes under UV illumination. (D) A TEM image of  $\text{Fe}_3\text{O}_4$  ( $6.4 \pm 0.5$  nm) forming a cavity-like structure in block copolymer assemblies. (E) An aqueous solution of block copolymer assemblies containing  $\text{Fe}_3\text{O}_4$  nanoparticles. The picture on the right shows assemblies attracted to a magnet. Scale bar is 100 nm.

nanoparticles acted as simple solutes. Indeed, most previous studies on the solution phase self-assembly have relied on the solubilization of nanoparticles in block copolymer assemblies.<sup>19,20</sup> Thus, little is known about the impact of nanoparticle loading on the self-assembly formation and the organization of nanoparticles in the self-assembled structure.

Recently, we have shown that the cooperative self-assembly of as-synthesized CdSe nanoparticles and PAA-*b*-PS can yield an unusual cavity-like assembly structure of nanoparticles in spherical block copolymer assemblies (Figure 1A).<sup>21</sup> This work showed that ordered arrays of nanoparticles can be formed by the solution phase self-assembly of nanoparticles and amphiphilic block copolymers. It also showed that nanoparticles can play an active role in the self-assembly process rather than being passively incorporated as a solute. Here, we demonstrate that the radial assembly is a general behavior for typical as-synthesized alkyl-terminated nanoparticles of varying sizes and reveal what drives the formation of the unique assembly structure. Furthermore, we present experimental and theoretical phase maps constructed for a range of different sized CdSe nanoparticles. These findings provide important practical guidelines for reproducibly fabricating nanoparticle/block copolymer hybrid materials with desired structures.

(21) Sanchez-Gaytan, B. L.; Cui, W. H.; Kim, Y. J.; Mendez-Polanco, M. A.; Duncan, T. V.; Fryd, M.; Wayland, B. B.; Park, S. J. Interfacial assembly of nanoparticles in discrete block-copolymer aggregates. *Angew. Chem., Int. Ed.* **2007**, *46*, 9235–9238.

## Results and Discussion

As described in Figure 1A, nanoparticles were incorporated into amphiphilic block copolymer micelles by slowly adding water to a *N,N*-dimethylformamide (DMF) solution of nanoparticles and block copolymers. The resulting coassemblies were then dispersed in water by dialysis and centrifugation and characterized by transmission electron microscopy (TEM). Amphiphilic block copolymers of poly(acrylic acid) and polystyrene (PAA<sub>38</sub>-*b*-PS<sub>154</sub>) were synthesized by the reversible addition–fragmentation chain transfer (RAFT) polymerization method<sup>21,22</sup> and used throughout the study. Zinc sulfide-coated cadmium selenide nanoparticles (CdSe@ZnS)<sup>23</sup> and iron oxide magnetic nanoparticles ( $\text{Fe}_3\text{O}_4$ )<sup>24</sup> were synthesized by literature procedures using trioctylphosphine oxide (TOPO) and oleic acid, respectively, as main surface coordinating ligands and used without further surface functionalization. Thus, all nanoparticles used in this study were terminated with hydrophobic alkyl molecules. Note that most literature procedures for organic phase synthesis of nanoparticles use surfactants terminated with a long alkyl chain as surface coordinating molecules.<sup>25</sup>

We have previously shown that TOPO-stabilized CdSe@ZnS nanoparticles and PAA-*b*-PS can self-assemble into well-defined spherical assemblies where nanoparticles form an unusual cavity-like structure as described in Figure 1A.<sup>21</sup> The phenomenon was general for a range of different sized CdSe@ZnS nanoparticles emitting green, yellow, and red light (Figure 1B,C).  $\text{Fe}_3\text{O}_4$  nanoparticles also formed the cavity-like structure inside block copolymer assemblies as shown in Figure 1D,E.<sup>26</sup> In all cases, block copolymers and nanoparticles self-assembled into a three-layered structure composed of a polymer core, a polymer shell, and nanoparticles arranged in-between the polymer core and the shell. The polymer structure of the radial assemblies resemble large compound micelles reported by Eisenberg and co-workers, which consist of one or more inverse micelles surrounded by a layer of PAA-*b*-PS.<sup>21,27</sup>

To examine the role of surface coordinating molecules on the formation of the radial assemblies, PS-modified  $\text{Fe}_3\text{O}_4$  nanoparticles were prepared by ligand exchange and self-assembled with block copolymers by following the same procedure. As shown in Figure 2A, the PS-modified nanoparticles were incorporated into block copolymer assemblies without any particular order. This is in contrast to the radial assembly formed with alkyl-terminated nanoparticles presented in Figure 2B. This result confirms that the relatively unfavorable interaction between alkyl-terminated nanoparticles and PS is responsible for the formation of the unusual radial coassemblies. Although alkyl-terminated nanoparticles and PS are both hydrophobic, the nanoparticle/PS interaction is unfavorable enough to cause the segregation of nanoparticles to the spherical PS/PS interface instead of being randomly incorporated

(22) Mayadunne, R. T. A.; Rizzato, E.; Chiefari, J.; Krstina, J.; Moad, G.; Postma, A.; Thang, S. H. Living polymers by the use of trithiocarbonates as reversible addition-fragmentation chain transfer (RAFT) agents: ABA triblock copolymers by radical polymerization in two steps. *Macromolecules* **2000**, *33*, 243–245.

(23) Peng, Z. A.; Peng, X. G. Formation of high-quality CdTe, CdSe, and CdS nanocrystals using CdO as precursor. *J. Am. Chem. Soc.* **2001**, *123*, 183–184.

(24) Sun, S. H.; Zeng, H. Size-controlled synthesis of magnetite nanoparticles. *J. Am. Chem. Soc.* **2002**, *124*, 8204–8205.

(25) Murray, C. B.; Kagan, C. R.; Bawendi, M. G. Synthesis and characterization of monodisperse nanocrystals and close-packed nanocrystal assemblies. *Annu. Rev. Mater. Sci.* **2000**, *30*, 545–610.

(26) Hickey, R. J.; Sanchez-Gaytan, B. L.; Cui, W. H.; Composto, R. J.; Fryd, M.; Wayland, B. B.; Park, S. J. Morphological Transitions of Block-Copolymer Bilayers via Nanoparticle Clustering. *Small* **2009**, *6*, 48–51.

(27) Zhang, L. F.; Eisenberg, A. Multiple morphologies and characteristics of “crew-cut” micelle-like aggregates of polystyrene-*b*-poly(acrylic acid) diblock copolymers in aqueous solutions. *J. Am. Chem. Soc.* **1996**, *118*, 3168–3181.

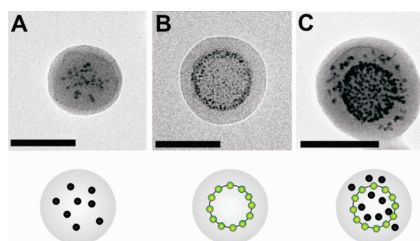


**Figure 2.** TEM images of block copolymer assemblies containing (A) PS-terminated  $\text{Fe}_3\text{O}_4$  nanoparticles ( $4.1 \pm 0.5$  nm), (B) alkyl-terminated  $\text{CdSe}@\text{ZnS}$  nanoparticles ( $4.6 \pm 0.4$  nm), and (C) both PS-terminated  $\text{Fe}_3\text{O}_4$  nanoparticles and alkyl-terminated  $\text{CdSe}@\text{ZnS}$  nanoparticles. The drawings showing the location of nanoparticles in the polymer matrix are given below the TEM images. Scale bar is 100 nm.

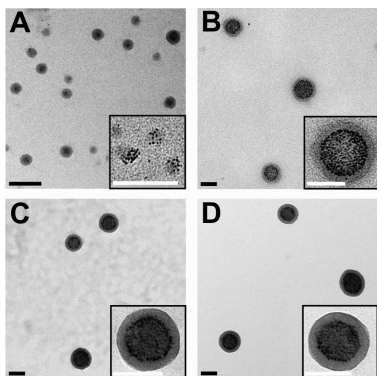


**Figure 3.** Coassemblies of  $\text{CdSe}@\text{ZnS}$  nanoparticles ( $4.1 \pm 0.4$  nm) and block copolymers formed at a series of different water content: 0% (A), 6% (B), 17% (C), and 100% (D). Scale bar is 100 nm.

throughout the polymer matrix. The incorporation of nanoparticles at the interface can also reduce the stretching penalty that would be incurred by incorporating them within the polymer core or in the shell. The distinct self-assembly behavior can be used to compartmentalize different types of nanoparticles within individual block copolymer assemblies. When PS-modified  $\text{Fe}_3\text{O}_4$  nanoparticles and alkyl-terminated  $\text{CdSe}@\text{ZnS}$  nanoparticles were simultaneously incorporated into block copolymer assemblies, alkyl-terminated  $\text{CdSe}@\text{ZnS}$  nanoparticles were localized at the spherical interface while PS-terminated  $\text{Fe}_3\text{O}_4$  nanoparticles were found throughout the assembly (Figure 2C) as confirmed by the energy dispersive X-ray spectroscopy (EDS) (Figure S1).

The radial coassembly process was monitored by taking TEM images at a series of different water contents. As shown in the TEM image presented in Figure 3A, TOPO-stabilized  $\text{CdSe}@\text{ZnS}$  nanoparticles are associated with block copolymers even before adding water due to the poor solubility of  $\text{CdSe}@\text{ZnS}$  nanoparticles in DMF. Initially, the system lowers the free energy by incorporating  $\text{CdSe}@\text{ZnS}$  nanoparticles in the PS domain of block copolymer aggregates because the TOPO/PS interaction is less unfavorable than TOPO/DMF interactions.<sup>28</sup> At this stage,  $\text{CdSe}@\text{ZnS}$  nanoparticles are incorporated into the swollen polymer aggregates without any particular order. With the addition of water, a selective solvent for the PAA block, the aggregation number of polymers becomes larger to avoid the contact

(28) The Flory–Huggins parameter for TOPO/PS (octane/PS = 9.0 MPa) is significantly smaller than all other interaction pairs (e.g., octane/PAA = 81.0 MPa, octane/DMF = 84.6), which means that TOPO/PS interaction is the least repulsive (most favorable) when compared with the other possible interactions.

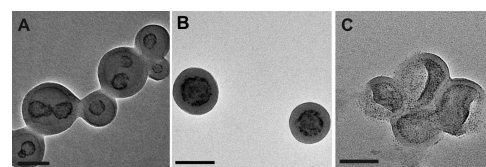


**Figure 4.** (A) Coassemblies of  $\text{CdSe}@\text{ZnS}$  nanoparticles ( $4.1 \pm 0.4$  nm) and block copolymers formed at different nanoparticle volume fractions, 0.012 (A), 0.035 (B), and 0.068 (C), representing the asymmetric assembly range (A), radial assembly range (B), and phase separation range (C), respectively. Scale bar is 100 nm.

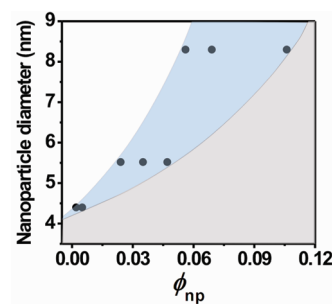


**Figure 5.** Nanoparticle volume fraction ranges yielding stable interfacial assemblies for different sized  $\text{CdSe}@\text{ZnS}$  nanoparticles (blue section). Experimentally determined data points are indicated with dots. The white section represents the asymmetric assembly range shown in Figure 4A, and the gray section represents the phase separation range.

between PS and water. As the polymer strands pack more densely, nanoparticles and polymers reorganize to adopt the radial assembly structure (Figure 3B–D). This observation also supports our hypothesis that the unusual radial coassembly structure is the result of relatively unfavorable interactions between nanoparticles and polymers.

The volume fraction of nanoparticles ( $\phi_{\text{np}}$ ) was found to be a critical factor in stabilizing the coassemblies, and the radial coassembly structure was formed for a limited range of nanoparticle volume fractions (Figures 4 and 5). When the nanoparticle volume fraction is larger than a threshold volume fraction ( $\phi_{\text{np}-\text{max}}$ ), nanoparticles and block copolymers macroscopically precipitate out of solution when dispersed in water. Figure 4C presents the assemblies formed at  $\phi_{\text{np}}$  slightly larger than  $\phi_{\text{np}-\text{max}}$ , which shows broken irregular assemblies. When  $\phi_{\text{np}}$  becomes even larger, massive aggregation and precipitation of nanoparticles and block copolymers occur. When  $\phi_{\text{np}}$  was too low, asymmetric assemblies with one or multiple nanoparticle cavities (Figure 4A) were formed instead of well-defined symmetric radial assemblies shown in Figure 4B. While the asymmetric assemblies have broad size distributions with different numbers of nanoparticle cavities, symmetric radial assemblies shown in Figure 4B were quite uniform with an average diameter of 130 nm and size distribution of 9% by TEM, which suggest that the resulting assembly is a thermodynamic structure. Consistent with this notion, a slower addition of water (10  $\mu\text{L}$  per 900 s) did not change the assembly structure.

The  $\phi_{\text{np}}$  ranges yielding well-defined symmetric radial coassemblies were identified for three different sized  $\text{CdSe}@\text{ZnS}$  nanoparticles which emit green, yellow, and red light (Figure 5). The diameters of the inorganic part of the nanoparticles were determined to be  $3.0 \pm 0.4$ ,  $4.1 \pm 0.4$ , and  $6.9 \pm 0.7$  nm by TEM. The nanoparticle diameters plotted in Figure 5 include the TOPO layer and were estimated by adding the TOPO layer thickness

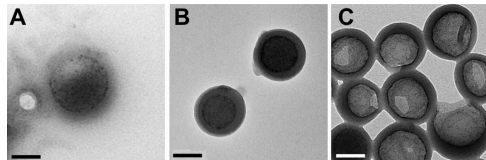


**Figure 6.** Coassemblies of CdSe@ZnS nanoparticles ( $3.0 \pm 0.4$  nm) and block copolymers in DMF/water mixtures at  $\phi_{\text{np}} = 0.024$ , which is larger than  $\phi_{\text{np\_max}}$  (0.01). The water contents are 12% (A), 17% (B), and 29% (C). The assemblies were macroscopically aggregated and precipitated out of solution when the water content was higher than 29%. Scale bar is 100 nm.

( $2 \times 0.7$  nm)<sup>29</sup> to the diameters determined by TEM. As shown in Figure 5, the volume fraction range that yields well-defined symmetric radial coassemblies (radial assembly range) varied with the size of nanoparticles. Larger nanoparticles required a higher nanoparticle volume fraction to form stable coassemblies and have a wider range of volume fractions that yield well-defined radial assemblies. In fact, it was difficult to form stable coassemblies with CdSe@ZnS nanoparticles smaller than 3.0 nm, as the radial assembly range becomes too narrow. When the nanoparticle volume fraction is larger than the radial assembly range, nanoparticles cannot effectively reduce the polymer stretching energy, which results in the phase separation of the two components with water addition (vide infra). The phase separation volume fraction range is indicated in gray in the phase map (Figure 5). Note that when the water content is low, coassemblies with well-defined layered structures are formed even at a nanoparticle volume fraction larger than  $\phi_{\text{np\_max}}$  (Figure 6B). As the water content is increased, however, nanoparticles and block copolymers were eventually aggregated and precipitated out due to the destabilization of the core region (Figure 6C). These observations imply that the polymer stretching is important in stabilizing the layered structure, which is supported by the theoretical study described below. Note that for homogeneous encapsulations, smaller nanoparticles are more readily incorporated because they have a less negative impact on the polymer conformation.<sup>30</sup>

To understand the formation of radial assemblies and the phase behavior further, we used a simple extension to the strong segregation theory of Olmsted and Milner<sup>31</sup> and calculated a phase map identifying nanoparticle volume fraction ranges where the core–shell structure with an interfacial nanoparticle layer has a lower free energy than such a structure without a nanoparticle layer. In the model, the only contributions to the free energy arise from chain stretching and the interfacial energy. Although a complete understanding of the physical processes may require calculations based on the self-consistent-field theory, the strong segregation theory has the advantage of permitting further analytical progress, which enables a qualitative understanding of the dominant processes governing structure formation in the complex systems considered here. In the calculation, it is assumed that the core is composed of a single spherical block copolymer reverse micelle, with the PAA on the inside of the sphere and PS on the outside (Figure 7). We expect that the core structure can be actually more complex and comprised of more than one reverse

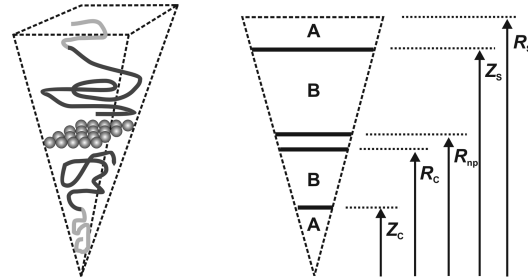


**Figure 7.** Schematic illustration of the wedge used to approximate a segment of the spherical core–shell structure with a nanoparticle layer at the interface. The dimensions used in the calculation are shown on the right. The radii,  $Z_c$  and  $Z_s$ , correspond to the distance from the center to the interfaces between the A and B blocks in the core and the shell, respectively. The  $R_c$  and  $R_s$  are the radii of the core and shell, and  $R_{\text{np}}$  is the radius of the inner surface of the shell, such that  $R_{\text{np}} = R_c + d_{\text{np}}$ , where  $d_{\text{np}}$  is the diameter of the nanoparticles.

micelle. We describe the nanoparticles as occupying a flat layer with thickness corresponding to that of the diameter of the nanoparticles,  $d_{\text{np}}$ ; thus, we neglect the possibility of partial packing of the layer and the impact that the curvature of the nanoparticles might have on the chain configurations at the copolymer/nanoparticle interface. Despite these simplifications, this model qualitatively reproduces the observed conditions required to stabilize the core–shell structure with a nanoparticle layer.

The free energy per chain,  $f_{\text{chain}}$ , corresponding to the core–shell structure is given by

$$\frac{1}{\Omega \gamma_{AB}/b} f_{\text{chain}} = \frac{V_c(f_{Ac}^{\text{str}} + f_{Bc}^{\text{str}} + f_c^{\text{int}}) + V_s(f_{As}^{\text{str}} + f_{Bs}^{\text{str}} + f_s^{\text{int}})}{V_c + V_s} \quad (1.1)$$

where  $\Omega$  is the volume of a single chain,  $\gamma_{AB}$  is the A/B (i.e., PAA/PS) interfacial tension, and  $b$  is a reference length scale, which we take to be equal to one nanometer. The volume of the core ( $V_c$ ) and the shell ( $V_s$ ) are related to the various radii defined in Figure 7 as  $V_c/(V_c + V_s) = R_c^3/(R_c^3 + R_s^3 - R_{\text{np}}^3)$  and  $V_s/(V_c + V_s) = (R_s^3 - R_{\text{np}}^3)/(R_c^3 + R_s^3 - R_{\text{np}}^3)$ . The subscripts, A, B, c, and s refer to block A, block B, the core, and the shell, respectively, and the superscripts str and int refer to stretching and interfacial energies. There are four contributions to the overall free energy per chain from chain stretching given by eqs 1.2–1.5, where  $\phi$  refers to the volume fraction of the A block.

$$f_{Ac}^{\text{str}} = \kappa \frac{(R_c/b)^2}{\phi^2} \int_0^{\beta_c} (\beta_c - y)^2 y^2 dy \quad (1.2)$$

$$f_{Bc}^{\text{str}} = \kappa \frac{(R_c/b)^2}{(1-\phi)^2} \int_0^{1-\beta_c} (\beta_c + y)^2 y^2 dy \quad (1.3)$$

$$f_{As}^{\text{str}} = \kappa \frac{(R_s/b)^2}{\phi^2 [1 - (R_{\text{np}}/R_s)^3]} \int_0^{1-\beta_s} (\beta_s + y)^2 y^2 dy \quad (1.4)$$

$$f_{Bs}^{\text{str}} = \kappa \frac{(R_s/b)^2}{(1-\phi)^2 [1 - (R_{\text{np}}/R_s)^3]} \int_0^{\beta_s - R_{\text{np}}/R_s} (\beta_s - y)^2 y^2 dy \quad (1.5)$$

(29) Jiang, J.; Krauss, T. D.; Brus, L. E. Electrostatic force microscopy characterization of trioctylphosphine oxide self-assembled monolayers on graphite. *J. Phys. Chem. B* **2000**, *104*, 11936–11941.

(30) Thompson, R. B.; Ginzburg, V. V.; Matsen, M. W.; Balazs, A. C. Predicting the mesophases of copolymer-nanoparticle composites. *Science* **2001**, *292*, 2469–2472.

(31) Olmsted, P. D.; Milner, S. T. Strong segregation theory of bicontinuous phases in block copolymers. *Macromolecules* **1998**, *31*, 4011–4022.

The parameters  $\beta_c$  and  $\beta_s$  are defined by

$$\begin{aligned}\beta_c &= z_c/R_c \equiv \phi^{1/3}; \quad \beta_s = z_s/R_s \\ &\equiv (1 - \phi(1 - (R_{np}/R_s)^3))^{1/3}\end{aligned}\quad (1.6)$$

Since we assume that the nanoparticle layer is filled with nanoparticles, we also have a further relation between  $R_s$  and  $R_c$

$$\phi_{np} R_s^3 = R_{np}^3 - R_c^3 \quad (1.7)$$

There are four contributions to the interfacial energy, two from each of the A–B interfaces, with an interfacial energy per unit area of  $\gamma_{AB}$ , and the other two from the B–nanoparticle interfaces. In the calculations presented below, we ignore the contributions from the latter since they are significantly smaller than the A–B interfacial energy.

$$f_c^{\text{int}} = 3 \frac{(z_c/b)^2}{(R_c/b)^3} \quad (1.8)$$

$$f_s^{\text{int}} = 3 \frac{(z_s/b)^2}{(R_s^3 - R_{np}^3)/b^3} \quad (1.9)$$

The dimensionless parameter,  $\kappa$ , in eqs 1.2–1.5 is defined by

$$\kappa = \frac{9\pi^2(l_A l_B)^{1/2}}{8\Omega^2 \gamma_{AB}} b^3 \quad (1.10)$$

where  $l_A$  and  $l_B$  are monomer segment lengths. Assuming that the monomer lengths are approximately the same ( $l_A \approx l_B = l$ ) and that the interfacial tension depends on the dimensionless polymer–polymer interaction parameter,  $\chi$ , as shown in eq 1.11<sup>32</sup>

$$\gamma \approx \left(\frac{\chi}{6}\right)^{1/2} l^{-2} \quad (1.11)$$

then  $\kappa$  can be written as

$$\kappa \approx \frac{9\pi^2\sqrt{6}}{8} \frac{1}{N^2 \chi^{1/2}} \left(\frac{b}{l}\right)^3 \quad (1.12)$$

where  $N$  is the degree of polymerization of the entire copolymer. The minimized total free energy was calculated for the self-assembled structure in order to determine whether the introduction of a nanoparticle layer lowers the free energy of the core–shell structure. The free energy for the core–shell structure without a nanoparticle layer is found by taking the limit of  $R_{np} \rightarrow R_c$  in eqs 1.2–1.9.

The calculated phase map is presented in Figure 8 where the blue shaded area represents the conditions where the radial coassemblies are stable. As mentioned above, the theoretical map reveals the same general trend observed in the experimental data in Figure 5. First, it indicates that radial coassemblies are stable for a limited range of nanoparticle volume fractions. When the nanoparticle volume fraction is too low, in the left side of the blue shaded region of the phase map, the inclusion of the nanoparticle layer destabilizes the assembly structure by

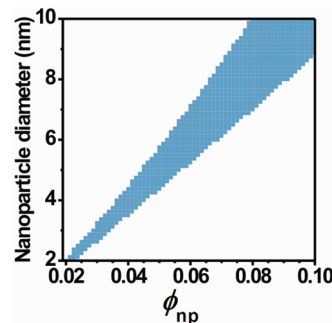


**Figure 8.** Calculated phase map in which the blue shaded region indicates the volume fraction ranges where the core–shell structure with a nanoparticle layer has a lower energy than the assemblies without the nanoparticle layer. The  $\kappa$  value of  $10^{-4}$  was used for the calculation.

increasing the stretching energy of the shell. Experimentally, the destabilization caused by the shell stretching is manifested by adopting the asymmetric structures shown in Figure 4A. When the nanoparticle volume fraction is larger than the radial coassembly range, the right side of the blue shaded region of the phase map, the inclusion of the nanoparticle layer destabilizes the assembly structure by increasing the stretching of the core. Experimentally, the nanoparticle-induced strain on the core stretching results in the phase separation of the nanoparticles and block copolymer with the addition of water (Figure 4C). In the blue shaded region, the nanoparticle layer has minimal impact on the dimensions of the polymer core and the shell. Furthermore, nanoparticles even relieve chain stretching, particularly in the shell, by reducing the curvature of the inner surface of the shell, stabilizing the coassembly structure. Second, the range of volume fractions over which the coassemblies are stable becomes broader as nanoparticle size increases because the stretching energy is relieved more significantly by incorporating larger nanoparticles. The calculated phase map along with the experimental data provides an essential guideline for the cooperative self-assembly of nanoparticles and block copolymers, from which one can determine the self-assembly conditions for encapsulating nanoparticles into discrete block copolymer assemblies.

## Conclusions

Nanoparticles can self-assemble into unique cavity-like structures in core–shell type assemblies of PAA-*b*-PS amphiphilic block copolymers. Initially, nanoparticles are randomly incorporated into the swollen aggregates of block copolymers in DMF. As polymers pack more densely with the addition of water, nanoparticles phase segregate to the spherical interface between the polymer core and the shell, forming a submicrometer nanoparticle cavity inside the polymer matrix. It was found that both the enthalpic interaction and the polymer stretching energy are important factors in the formation of radial coassemblies. The slightly unfavorable interaction between alkyl-terminated nanoparticles and the hydrophobic segment of polymers (i.e., PS) causes the segregation of nanoparticles to the interface between the polymer core and the shell. PS-modified nanoparticles, on the contrary, were randomly incorporated into block copolymer micelles without a particular order because of the favorable interaction between nanoparticles and polymers. Strong segregation theory calculations along with corresponding experimental data revealed that the polymer stretching is also important in forming the layered structure. Because of the polymer stretching energy, coassemblies were stabilized for limited nanoparticle

(32) Helfand, E.; Tagami, Y. Theory of Interface between Immiscible Polymers. *J. Polym. Sci., Part A: Polym. Chem.* **Lett.** *1971*, **9**, 741.

volume fractions where the inclusion of nanoparticle layers reduces the polymer stretching and lowers the free energy of coassemblies. In addition, the range of volume fractions required for the coassembly varied sensitively with nanoparticle size. Because bigger nanoparticles can relieve stretching energy more effectively, the working volume fraction range became broader with increasing the nanoparticle size. The experimentally determined phase map along with the theoretical calculation provides the self-assembly conditions required to stabilize the coassembly structure of as-synthesized alkyl-terminated nanoparticles and block copolymers.

## Methods

### Preparation of Coassemblies of Nanoparticles and Block Copolymers.

Nanoparticles and block copolymers were self-assembled as described previously.<sup>21</sup> In a typical experiment, 25  $\mu$ L of a PAA<sub>38</sub>-*b*-PS<sub>154</sub> solution ( $1.6 \times 10^{-4}$  M) in DMF was mixed with 25  $\mu$ L of a ZnS-coated CdSe nanoparticle solution ( $1.6 \times 10^{-6}$  M) in chloroform. While stirring, 1 mL of DMF is added to the solution followed by a slow addition of 300  $\mu$ L

of water (18 M $\Omega$ ·cm) at a rate of 10  $\mu$ L per 30 s. The mixture was kept under stirring for 12 h before adding additional water (1.5 mL) over 15 min. Then, the samples were dialyzed against water for 24 h and further purified by a series of centrifugations. The volume fraction of nanoparticles is defined by the total volume of nanoparticles over the combined volume of the nanoparticles and block copolymer. The volume fraction of nanoparticles was varied by changing the amount of nanoparticles while keeping the amount of block copolymer constant.

**Acknowledgment.** This research was supported by the MRSEC seed award (DMR 05-20020), NSF career award (DMR 0847646), ARO young investigator award (W911NF-09-1-0146), and the Nano/Bio Interface Center through the National Science Foundation IGERT DGE02-21664.

**Supporting Information Available:** Detailed experimental procedures for the synthesis of block copolymers and nanoparticles and EDS data showing the location of nanoparticles in block copolymer assemblies. This material is available free of charge via the Internet at <http://pubs.acs.org>.